Desalination and Water Treatment
www.deswater.com

doi: 10.1080/19443994.2015.1052994

57 (2016) 12443–12452
June

Taylor & Francis
Taylor & Francis Group

Preparation of novel diatomite-based composites: applications in organic effluents sorption

Nedjma Khelifa[a,b,c,*], Jean-Philippe Basly[c], Boualem Hamdi[a,b], Michel Baudu[c]

[a]*Ecole Nationale Supérieure des Sciences de la Mer et de l'Aménagement du Littoral, BP 19, Bois des cars, DelyIbrahim, Alger, Algeria, Tel. +213 559 340 999; email: khelifa_nedj@yahoo.fr (N. Khelifa), Tel. +213 5550601743; email: bhamdi_99@yahoo.fr (B. Hamdi)*

[b]*LPCMAE, Faculté de Chimie, USTHB, BP 32 El Alia Bab Ezzouar, 16111 Alger, Algeria*

[c]*Groupement de Recherche Eau Sol Environnement (EA 4330 GRESE), Université de Limoges, 123 Avenue Albert Thomas, 87060 Limoges, France, Tel. +33 555 43 58 98, Tel. +33 555457367; email: jean-philippe.basly@unilim.fr (J.-P. Basly), michel.baudu@unilim.fr (M. Baudu)*

Received 17 February 2015; Accepted 10 May 2015

ABSTRACT

A new diatomite-based composite is prepared and used for environmental remediation. The Algerian diatomite has been used for the first time for this application. Preparation conditions showed increased surface area with improved sorption properties. This composite consisting of diatomite (Dia) and activated carbon (C) was prepared using a mixture of diatomaceous earth and glucose. Effects of thermal and chemical treatments are studied. methylene blue (MB), methyl orange (MO) and para-nitro-phenol (PNP) from aqueous solution were chosen as pollutants to test retention capacity. Physical, chemical and structural properties of these new hybrid materials have been investigated by several methods. The surface areas of pure and modified diatomite are estimated to be (22 $m^2 g^{-1}$) and (100–173 $m^2 g^{-1}$), respectively. Sorption kinetics and isotherms for MB, MO and PNP were carried out in order to determine their respective adsorption capacity. The surface charges (negatives) and macroporosity of diatomite did not allow the adsorption of PNP and MO. However, modified diatomite (Dia/C) showed ability to eliminate these pollutants, despite their dominant inorganic nature. The pseudo-second-order kinetics and the Langmuir model described sorption data reasonably well. The study showed that the composite materials can be used as potential efficient sorbents.

Keywords: Diatomite; Activated carbon; Composite materials; Thermal treatment; Chemical treatment; Characterization; Adsorption; Dyes

1. Introduction

Synthetic dyes are increasingly used in the textile, paper and plastics materials. Many industries use the dyes in order to colour their products, thereto, consumes substantial volumes of aqueous solutions which will then potentially pollute water resources after their release. Colour change is the first contamination sign of released water [1]. P-Nitrophenol is a chemical compound that has a hydroxyl group and a nitro group [2,3]. These groups are attached to a benzene ring relatively in para position.

*Corresponding author.

Para-Nitro-Phenol (PNP) is an important intermediate in the manufacturing of azo dyes [4]. So, PNP also occurs as contaminants of industrial effluents. The presence of very small amounts of dyes in water (less than 1 ppm for some dyes) is highly visible and undesirable [1,5].

The treatment of effluents has become a challenging topic in environmental sciences, because of the complexity of the required purification processes and methods. Besides capital cost, required consumables (e.g. adsorbents cost) make effluent treatment quite expensive in numerous cases. The simplicity of the pollutants adsorption process makes it an increasingly important in purification and separation at the industrial scale. Activated carbon is one of the most widely used adsorbent in industry. However, carbon adsorption technology is still an expensive process. In the recent years, this has prompted a growing research interest into the low-cost alternatives for the production of activated carbon materials on new generation of hybrid-based mineral composite such as diatomite that can be applied to water treatment [6–10].

The main component of diatomite is SiO_2, with a relatively small percentage of other oxides such as Al_2O_3, Fe_2O_3, MgO, CaO and others. The total content varies depending on source; the Algerian diatomite is particularly polluted by a high rate of calcium carbonates that can exceed 10%.

Diatomite, also referred as diatomaceous earth, is a soft lightweight pale coloured sedimentary rock available in large deposits around the world and widely used in industry [11–13]. It consists of silica microfossils of aquatic unicellular alga varying in shape and size of diatom (typically 10–200 μm) [14]. The porous structure, the low density, the high surface area [15–21] and the low cost [22] make the diatomite and the treated diatomite, good sorbent candidates. The diatomite is known to show good adsorbent properties towards inorganic pollutants and basics dyes [15–21].

The microporous and hydrophobic structure of the carbon matrix allows good adsorption properties towards non-polar molecules. Thus, the complementarily of these two components may give raise to hybrid composite materials with optimal separation properties for a wide range of pollutants. Thus, the Dia/C composite could be of high interest for some specific applications such as separation and purification purposes [14,20,23–31].

The high adsorptive capacities of activated carbons are related to properties such as surface area, pore volume and porosity. These unique characteristics are dependent on the type of raw materials employed and the method of activation. The manufacturing process of activated carbons involves two steps: the carbonization of raw carbonaceous materials in an inert atmosphere and the chemical–physical activation of carbonized product.

In previous works [29–31], composites were prepared from a mixture of diatomite and local charcoal using pyrolysis, and were tested against p-cresol [30] and heavy metals [31]. *In situ* production of activated carbon may reduce the overall cost. Furthermore, the porous textures could be tuned as function of the preparation conditions [32].

The main objective of this study is the synthesis of diatomite/carbon composites, (where carbon was prepared "*in situ*" from glucose), using thermal [33] and/or chemical [34] activation treatments. For the first time, Algerian diatomite will be used for preparing these composites and tested. This approach is expected to improve purification efficiency while using a biomass source for the carbon component [35]. To better understand the effect of preparation conditions, detailed testing and physicochemical characterizations have been carried out in parallel in this work and reported in this paper. Specifically, sorption properties were evaluated using a cationic dye methylene blue (MB), an anionic dye methyl orange (MO) and a neutral organic pollutant 4-nitrophenol (4-NP) from diluted aqueous solutions. The adsorption performance of the hybrid composites was evaluated and compared to diatomaceous earth.

2. Experimental part

2.1. Materials

A raw diatomite sample, (called KNT hereafter [28–30]), from the Sig deposit located in the westward of Algeria was used as starting material. The chemical composition (wt%) of this white porous material is 78.4 (SiO_2), 11.1 (CaO), 2.5 (Al_2O_3) and 1.3 (Fe_2O_3). The diatomite is grinded then sifted until obtaining homogenous powders with grain sizes lower than 50 μm. Diatomite (50 g) and glucose (50 g) were dry blended before adding water (10 mL) to form an homogeneous paste which was then dried (80°C), grinded and sieved. Four composite materials called $(Dia/C)_t$, $(Dia/C)_c$, $(Dia/C)_{ct}$ and $(Dia/C)_{tc}$ were prepared by thermal, chemical, chemical followed thermal and thermal followed by chemical of this mixture, respectively (Table 1). From the raw diatomite, four activated diatomite without incorporation of carbonaceous materials, referred by KNT_t, KNT_c, KNT_{ct} and KNT_{tc}, were also prepared and used as references.

During thermal treatment, the mixture is exposed to an inert N_2 gas flow up to 850°C with heating speed equal to 15°C/min and left for 1 h at the final

Table 1
Characteristics of the different materials used in this study

Symbol	Starting from	First treatment	Second treatment
KNT	KNT	–	–
Dia/C	KNT/glucose	–	–
$(KNT)_t$	KNT	Thermal	–
$(Dia/C)_t$	Dia/C	Thermal	–
$(KNT)_c$	KNT	Chemical (H_2SO_4)	–
$(Dia/C)_c$	Dia/C	Chemical (H_2SO_4)	–
$(KNT)_{ct}$	KNT	Chemical (H_2SO_4)	Thermal
$(Dia/C)_{ct}$	Dia/C	Chemical (H_2SO_4)	Thermal
$(KNT)_{tc}$	KNT	Thermal	Chemical (HCl)
$(Dia/C)_{tc}$	Dia/C	Thermal	Chemical (HCl)

temperature. The acid (chemical) treated samples were obtained using HCl 0.5 N/concentrated H_2SO_4. In the case of H_2SO_4 treatment, glacial sulphuric acid was added to the same starting mixture. The resulting mixture is left covered for 24 h at room temperature and then dried in an oven at 30°C.

For the HCl treatment, after the thermal treatment, the material is subjected to an HCl treatment. The mixture is then placed in a flask fitted with a condenser; the resulting reaction mixture is maintained at 100°C for 6 h. Following acid reaction, materials are rinsed with distilled water until the washing water reaches a neutral pH. Resulting samples are dried overnight at 110°C and then preserved in hermetically closed bottles before their use.

2.2. Characterization

The X-ray diffraction patterns were obtained using a PAN Analytical X-PERT PRO X-ray powder diffractometer (Cu Kα radiation, $\lambda = 1.5418$ Å, 45 kV). The indexation and phase identification were determined using X'pert Highscore plus Panalytical software. Nitrogen sorption properties were measured using a Micromeritics Sorb II 2300. Specific surface area was calculated from the Brunauer–Emmett–Teller (BET) equation. Microstructure and morphology of the materials were recorded by SEM on a Philips XL 30 (accelerating voltage of 15 kV). FTIR spectroscopy (using a Perkin Elmer spectrum 65 FTIR spectrometer) was performed in the 4,000–400 cm^{-1} range to identify the chemical functional groups present in the samples. The FTIR sample was obtained after finely grounding and dispersion into KBr powder-pressed pellets. Zeta potentials were measured with a Zetaphorometer IV (CAD Instruments) using at least three different samples.

2.3. Adsorption experiments

MB, MO and 4-nitrophenol (4-NP) stock solutions (1 g L^{-1}) were prepared by shaking in Milli-Q water and buffered at pH 5.5 at room temperature. Kinetic studies were conducted in brown flasks at room temperature by shaking 0.1 g of sorbent at 260 rpm on a mechanical shaker (EDMUND BUHLER GmbH SM-30), with 100 mL of 50 mg L^{-1} solution containing MB, MO or 4-NP. The samples were withdrawn from the shaker at intervals from 0 to 1,440 min. Isotherms were determined by shaking different amounts of adsorbents (varying from 25 to 500 mg) with 100 mL of 50 mg L^{-1} solution containing MB, MO or 4-NP for 24 h. After filtration through a 0.45-μm membrane, samples concentrations for kinetic and isotherms experiments were determined by UV–Visible spectrophotometry on a CARY 50 Probe (Varian spectroscopy instruments) at $\lambda = 318$ nm (4-NP), 505 nm (MO) and 664 nm (MB).

Modelization of the adsorption data was performed by non-linear regression analysis using STATISTICA 6.0 software on a Windows XP platform. The suitability was assessed on the basis of R^2. Kinetic data were fitted using a pseudo-second-order model following previous works [29,30], (Eq. (1)):

$$q(t) = \frac{qeq^2 K_2 t}{1 + q_{eq} K_2 t} \quad (1)$$

With q_{eq} the amount of the pollutant adsorbed at equilibrium (mg g^{-1}), q (t) the concentration of pollutant at time t and K_2 is the pseudo-second-order rate constant (g mg^{-1} min^{-1}).

Isotherms data [29,30] were fitted using a Langmuir model (Eq. (2)):

$$q_{eq} = q_{max} \frac{K_l Ce}{1 + K_l C_e} \quad (2)$$

where q_{eq} (mg g^{-1}), C_e (mg L^{-1}), q_{max} (mg g^{-1}) and K_L (L mg^{-1}) are the amount of the pollutant adsorbed at equilibrium, equilibrium concentrations, the Langmuir constants related to the sorption capacity and energy, respectively.

3. Results and discussion

3.1. Characterization of composites

Measurements with scanning electron microscopy (SEM) showed that the diatom shells are disk-shaped and relatively uniform in diameter (Fig. 1). The average size of these diatoms is estimated at 40 μm. A highly developed porous structure with a pore size of 1–2 μm could be also inferred from images. The treatments seem to open more pores of natural diatomite and reduce its thickness (Fig. 1).Further investigation has also shown the adhesion of silica (Kieselguhr) with the carbonaceous product. This indicates the carbon materials deposition as well as a uniform distribution on the porous matrix surface (Fig. 1). The carbon coating on $(Dia/C)_{ct}$, is very thin because the macropores are clearly identifiable on the surface of the composite probably due to acid attack.

A characteristic of the Algerian diatomite used in this study is its high level of carbonate and the treatments induced a colour modification of the material. The KNT is pale yellow before any treatment. The FTIR spectrum of natural diatomite (Fig. 2(A)) showed adsorption bands assigned to symmetric stretching of Si–O–Si (470, 695 and 800 cm^{-1}) [36], carbonate (calcite) v2-out of plane symmetric stretching (875 cm^{-1}) [37], asymmetric stretching vibrations of the siloxane group Si–O–Si (1,095 cm^{-1}) [36,38,39], carbonate (calcite) v3-asymmetric stretching (1,430 cm^{-1}) [37] physically bonded water (1,640 cm^{-1}) [26,28–30] and free silanols groups (3,400–3,600 cm^{-1}) [36,38–40]. Changes which occur in the FTIR spectra upon treatments are noteworthy. When thermal treatment is applied, a drastic decrease in H_2O bands intensity and in the specific calcite vibrations (marked by a circle in Fig. 2(A)). The chemical treatment did not remove completely the water-related peaks. The calcite vibration peaks were totally removed by the (single)

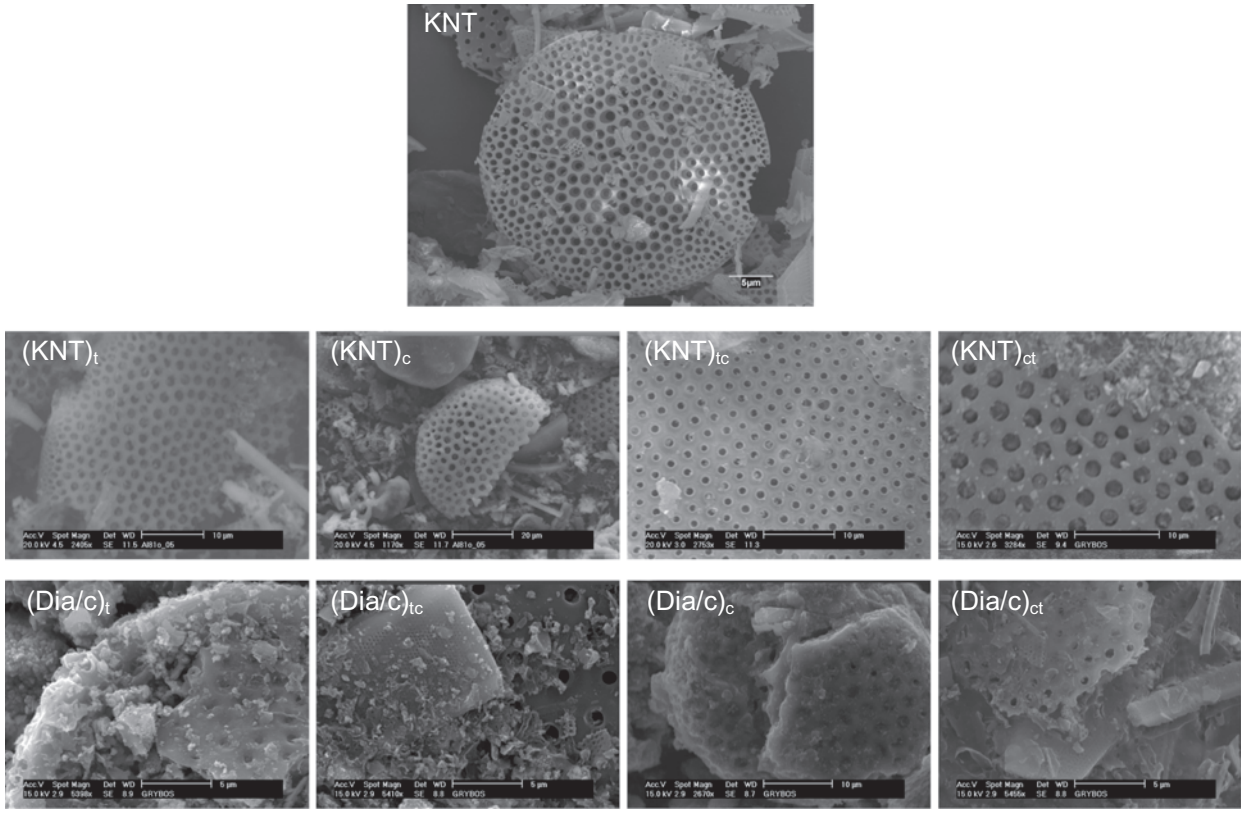

Fig. 1. Scanning electron microscope image of raw the diatomite (KNT), the treated diatomite $(KNT)_t$, $(KNT)_c$, $(KNT)_{tc}$, $(KNT)_{ct}$ and the diatomite/carbon composites $(Dia/c)_t$, $(Dia/c)_c$, $(Dia/c)_{tc}$, $(Dia/c)_{ct}$.

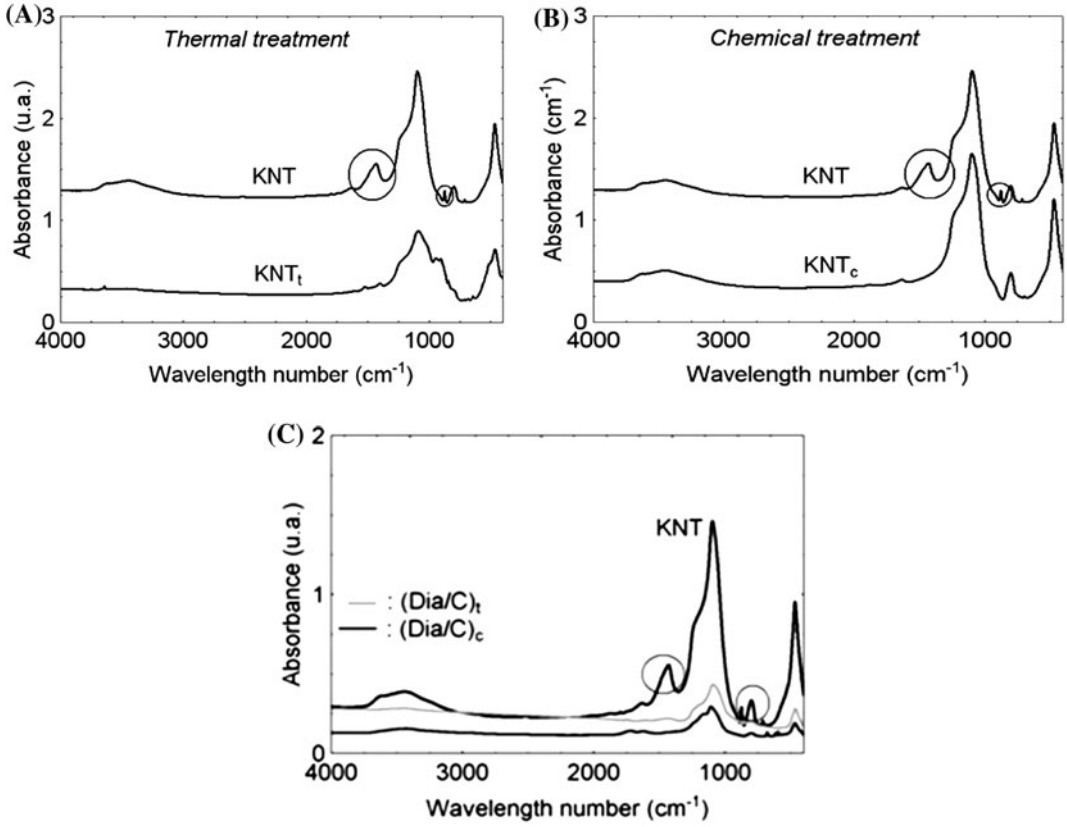

Fig. 2. FTIR spectra of (A) natural diatomite KNT and thermally activated KNT$_t$, (B) KNT and chemically activated KNT$_c$, and (C) KNT and the diatomite/carbon composites (Dia/C)$_t$, (Dia/C)$_c$. Circles show the calcite stretching vibration peaks.

chemical treatment (Fig. 2(B)). Combinations of thermal and chemical treatment have reduced significantly the Si–O–Si-related peaks. Note that the weak absorbance peaks of the carbon phase [41] were not observed on the FTIR spectra of the diatomite/carbon composite materials (Fig. 2(C)).

Fig. 3 shows the effect of the different treatment on the raw and modified diatomite materials. It is clear that the diffraction patterns related to silica are not significantly modified by the different treatments. This indicates that the starting raw materials (KNT) have a high resistance to the different treatments. Chemical treatment of the raw diatomite (KNT$_c$ in Fig. 3(A)) increases the amorphous phase, while calcite disappeared in accordance with the FTIR results. Thermal treatment does not totally remove the calcite from the raw diatomite (KNT$_t$ in Fig. 3(A)). Action of successive activation processes lead to XRD spectra similar to the last activation process (Fig. 3(B)).The carbonaceous material layer gives raise to two broad XRD diffractions peaks, observed at 22° and 45°, and attributed to $\langle 0\,0\,2\rangle$ and $\langle 1\,0\,0\rangle$ reflections [42], respectively (Fig. 3(C)). The graphitization degree of carbon is related to the crystallite size d estimated from the (0 0 2) peak width [42]. A value of $d = 0.411$ nm is obtained. This value is larger than that of the ideal graphite (0.335 nm) [43] indicating that the carbonaceous material layer was formed with some degree of disorder [44]. Successive chemical and thermal treatment of diatomite/glucose mixture enhances the amorphization (Fig. 3(D)).

Following chemical modification, the specific surface area of the diatomite significantly decreases indicating important structural changes and possibly a lower potential adsorption capacity. The total pore volume of diatomite decreased, due to structural changes. A similar observation was reported elsewhere [45–47].

The treatment processes (carbonization) promote the increase in the surface area and the development of the structure for (Dia/C)$_c$, (Dia/C)$_t$ and (Dia/C)$_{tc}$ materials. In the case of (Dia/C)$_{ct}$, the surface characteristics of the pores are not different from the raw diatomite. This corroborates the results of the XRD where an increase in amorphous phase has been observed. An increase in BET surface area from

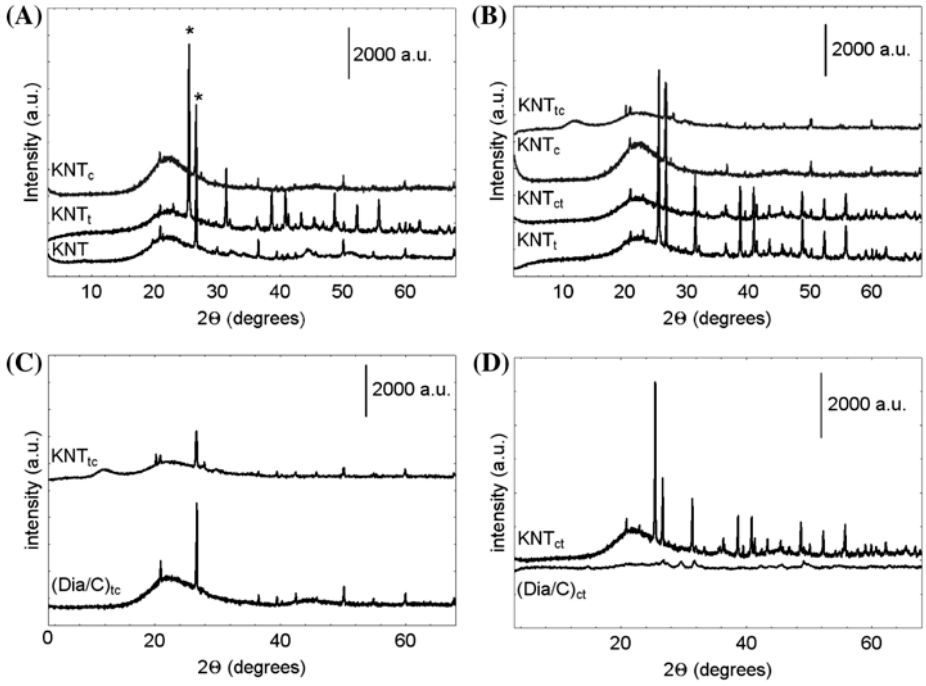

Fig. 3. X-ray diffraction pattern obtained from (A) KNT, KNT_t and KNT_c, (B) KNT_t, KNT_{ct}, KNT_c and KNT_{tc}, (C) KNT_{tc} and $(Dia/C)_{tc}$, and (D) KNT_{ct} and $(Dia/C)_{ct}$.

20.120 $m^2\ g^{-1}$ (raw Diatomite) to 110.469, 148.836,173. 435 and 21.732 $m^2\ g^{-1}$ has been measured for $(Dia/C)_{tc}$, $(Dia/C)_t$, $(Dia/C)_c$ and $(Dia/C)_{ct}$, respectively. A more detailed comparison of the surface area and pore volume for the raw and modified diatomite is shown in Table 2.

The zetametry provides information regarding the transition from the negative charged layer to the positive charged layer on the surface of materials. We have found that at low pH, the isoelectric value (pH_{ie}) increases from 1.7 to 3 following treatement of the raw diatomite (Table 2).

Zeta potential was modified with the activation processes [46]. When pH is decreased in a basic solution, more positive charges were added until the isoelectric point is reached at pH around 3.0. Given that the diatomite surface is naturally negatively charged, acid activation will give raise to positively charged material. Thermal activation and followed by acid activation will thus create even more charges in accordance with previously results [24,48].

A single activation gives raise to carbon phase within the diatomaceous earth matrix. The second activation process improves carbon adhesion and

Table 2
Physical characteristics of the different materials used in this study. Surface area (S), pore volume (V) and isoelectric potential are provided

Material	S^a_{BET} ($m^2\ g^{-1}$)	S^b_e ($m^2\ g^{-1}$)	S^c_p ($m^2\ g^{-1}$)	V^d_p ($cm^3\ g^{-1}$)	pH_{iep}
KNT	20	14	6	0.003	–
$(Dia/C)_c$	173	71	102	0.044	1.7
$(Dia/C)_t$	110	28	82	0.042	<2
$(Dia/C)_{tc}$	149	32	117	0.063	2.7
$(Dia/C)_{ct}$	22	3	19	0.01	1.8

Notes: $(Dia/C)_x$ series were prepared with addition of glucose on diatomite (where x is their treatment), respectively. t, c, tc and ct correspond, respectively, to the treatment thermal, chemical, both of (thermal and chemical) and both of (chemical and thermal). a: surface BET area; b: external surface; c: micropore area; d: micropore volume; pH_{ie}: pH isoelectric.

removes impurities embedded during the first activation stage. However, characterizations showed poor performance of the material which undergoes the second thermal activation in the case of $(Dia/C)_{ct}$. This is due to the high-rate formation of amorphous phase with small specific surface area.

3.2. Kinetics of adsorption from solutions

The relative retention properties of MB, MO and PNP on the raw diatomite (KNT) have been evaluated. Only MB is found to adsorb effectively. Data do not indicate any sign of adsorption in the case of neither MO nor PNP. We studied the kinetic evolution (not shown) of the adsorption of the (MB, MO and PNP) on the differents adsorbents and fitted the results to the second-order kinetic model (Table 3). The negative surface charge of raw KNT under neutral/alkaline pH values favours the sorption of cationic species and weak capacities were determined (<2 mg g^{-1}) for the anionic dye (MO) and the neutral phenolic pollutant (4-nitrophenol) (Table 3). Ho and Mckay's pseudo-second-order model Eq. (3) [49] is used to describe the kinetics

$$\frac{t}{qt} = \frac{1}{K_2 q_{eq}^2} + \frac{t}{q_{eq}} \quad (3)$$

With K_2 the rate constant of sorption (g mg^{-1} min^{-1}), q_{eq} is the amount of the pollutant adsorbed at equilibrium (mg g^{-1}) and q_t is the amount of the pollutant adsorbed at any time t (mg g^{-1}).

This model predicts the effect over the whole adsorption range. It was shown that the adsorption mechanism is the limiting stage, not the mass transport [50,51].

The calculated pseudo-second-order constant for all molecules showed some significant different between the different molecules (Table 3). The thermal or chemical treatment of (Dia/C) increases the reactivity and the affinity of composites materials for the three pollutants. However, activation is more favourable for the kinetic adsorption of MB.

3.3. Isotherms

Following the kinetic experiments, the equilibrium adsorption isotherms were obtained.

The results show that the adsorption balance when using differents masses of the produced activated carbons in liquid phase at initial concentration of pollutants in water.The isotherms (Fig. 4) can be classified as L-2 type according to the classification suggested by Giles et al. [52]. This indicates that the adsorption process is stimulated. Langmuir isotherms which indicate a homogenous [53] distribution of active sites on the surface with monolayer surface coverage of organic compounds fit well with the results (Fig. 4).

The adsorption results (Table 4) showed that adsorbent ($(Dia/C)_c$) has a higher capacity for removing MB. This is attributed to higher active sites (positive ions) in ($(Dia/C)_c$) which can react with the functional groups of MB. This reaction may lead to some complex formation. It is worth noting that basic dye adsorption capacity of activated carbon depends not only on the BET surface area, but also interaction of positive ions with surface functional groups of activated carbons [54,55]. While the activated carbon ($(Dia/C)_{tc}$) has a higher capacity for removing MO and PNP. Results shown in Table 4 point out that all pollutants were adsorbed in a greater extent on the

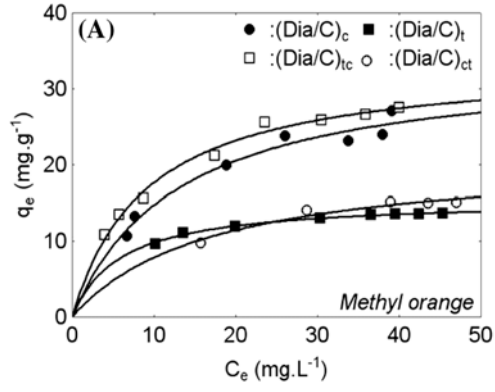

Fig. 4. Methyl orange adsorption isotherms obtained on the different diatomite/carbon composites.

Table 3
Kinetics pseudo-second-order parameters obtained for PNP, MB and MO by composit materials

Materials	$(Dia/c)_c$	$(Dia/c)_t$	$(Dia/c)_{tc}$	$(Dia/c)_{ct}$
K_2 (4-nitrophenol PNP)	(1.1 ± 0.2) 10^{-3}	(7.4 ± 0.8) 10^{-4}	(6.1 ± 0.7) 10^{-5}	–
K_2 (Methylene blue MB)	(6.6 ± 1.0) 10^{-6}	(1.6 ± 0.2) 10^{-4}	(4.5 ± 0.9) 10^{-3}	(5.4 ± 0.7) 10^{-4}
K_2 (Methyl orange MO)	(3.2 ± 0.4) 10^{-5}	(2.5 ± 0.3) 10^{-5}	(1.0 ± 0.2) 10^{-5}	(6.2 ± 0.5) 10^{-4}

Note: K_2 is expressed in L mg^{-1} mn^{-1}.

Table 4
Langmuir constants of MO, MB, PNP biosorption by composit materials

	$(Dia/C)_c$	$(Dia/C)_t$	$(Dia/C)_{tc}$	$(Dia/C)_{ct}$
Methyl orange (MO)				
q_{max} (mg g^{-1})	33.8 ± 2.4	15.5 ± 0.2	33.6 ± 1.1	21.2 ± 1.9
K_L	(7.6 ± 1.5) 10^{-2}	(17.1 ± 1.0) 10^{-2}	(11.1 ± 1.1) 10^{-2}	(5.9 ± 1.6) 10^{-2}
R^2	0.960	0.989	0.987	0.941
Methylen blue (MB)				
q_{max} (mg g^{-1})	63.4 ± 0.8	27.5 ± 0.8	25.6 ± 0.9	95.3±19.8
K_L	(5.2 ± 0.3) 10^{-1}	(2.6±0.4) 10^{-1}	(25.6 ± 5.2) 10^{-1}	(0.17 ± 0.05) 10^{-1}
R^2	0.997	0.967	0.959	0.989
4-Nitrophenol (PNP)				
q_{max} (mg g^{-1})	63.6 ± 5.5	34.3 ± 3.0	63.8 ± 7.4	38.6±1.7
K_L	(2.7 ± 0.05) 10^{-1}	(2.7 ± 0.2) 10^{-1}	(2.1 ± 0.1) 10^{-1}	(2.37 ± 0.45) 10^{-1}
R^2	0.924	0.910	0.937	0.968

carbon samples than on the raw precursor materials. Indeed, carbonization of diatomite leads to materials able to remove anionic dye (MO) and neutral phenolic pollutant (4-nitrophenol) from aqueous media.

4. Conclusion

The objective of this work is to develop, characterize and apply new hybrid composite materials, using for the first time a mixture of Algerian diatomaceous earth and glucose as carbon precursors (Dia/C). This could represent a cost-effective alternative to current commercial technologies for organic and inorganic pollutants. The retention properties of these novel composites have been optimized through different materials treatments.

In this work, a series of activated carbons composites were prepared from single or combination of treatments. These novel materials have been tested for their retention capacity for some environmental pollutants. The pollutants chosen in this study are MB, MO and 4-nitrophenol (PNP).

Using SEM and the gas adsorption techniques, we showed the formation of a carbon film on the silicic matrix with a porous texture. The high specific surface gives raise to a mesostructure. The operating conditions used for the diatomite treatments have not only led to structural and textural changes but also to change in the chemical properties of the starting materials.

We have also observed that the retention of polutants in the composites materials is controlled by the pseudo-second-order model. On the other hand, the adequacy of the model of Langmuir adsorption of the three pollutants, revealed specific adsorption, without adsorbate–adsorbate interactions.

All these results demonstrate that despite their low porosity, Algerian diatomite is cost-effective matrix material for the removal of aromatic (non-polar) and dyes (acidic and basic), and their use in remediation of polluted streams.

References

[1] I.M. Banat, P. Nigam, D. Singh, R. Marchant, Microbial decolorization of textile-dyecontaining effluents: A review, Bioresour. Technol. 58 (1996) 217–227.
[2] W. Mulbry, J. Karns, Purification and characterization of three parathion hydrolases from gram-negative bacterial strains, Appl. Environ. Microbiol. 34 (1989) 809–813.
[3] A. Schackmann, R. Muller, Reduction of nitro aromatic compounds b different *Pseudomonos* species under aerobic conditions, Appl. Microbiol. Biotechnol. 34 (1991) 809–813.
[4] O.I. Guliy, O.V. Ignatov, O.E. Makarov, V.V. Ignatovet, Determination of organophosphorus aromatic nitro insecticides and p-nitrophenol by microbial-cell respiratory activity, Biosens. Bioelectron. 8 (2008) 1005–1013.
[5] T. Robinson, G. McMullan, R. Marchant, P. Nigam, Remediation of dyes in textile effluent: A critical review on current treatment technologies with a proposed alternative, Bioresour. Technol. 77 (2001) 247–255.
[6] K.M. Doke, E.M. Khan, Adsorption thermodynamics to clean up wastewater; critical review, Rev. Environ. Sci. Biotechnol. 12 (2013) 25–44.
[7] A. Bhatnagar, M. Sillanpää, Utilization of agro-industrial and municipal waste materials as potential adsorbents for water treatment—A review, Chem. Eng. J. 157 (2010) 277–296.
[8] A. Demirbas, Agricultural based activated carbons for the removal of dyes from aqueous solutions: A review, J. Hazard. Mater. 167 (2009) 1–9.
[9] V. Nurchi, I. Villaescusa, Agricultural biomasses as sorbents of some trace metals, Coord. Chem. Rev. 252 (2008) 178–188.

[10] G. Crini, Recent developments in polysaccharide-based materials used as adsorbents in wastewater treatment, Prog. Polym. Sci. 30 (2005) 38–70.
[11] J.F. Lemonas, Diatomite, Am. Ceram. Soc. Bull. 76 (1997) 92–95.
[12] Z. Korunic, Diatomaceous earths, a group of natural insecticides, J. Stored Prod. Res. 34 (1998) 87–97.
[13] M. Bessho, Y. Fukunaka, H. Kusuda, T. Nishiyama, High-grade silica refined from diatomaceous earth for solar-grade silicon production, Energy Fuels. 23 (2009) 460–465.
[14] W.T. Tsai, H.C. Hsu, T.Y. Su, K.Y. Lin, C.M. Lin, Removal of basic dye (methylene blue) from wastewaters utilizing beer brewery waste, J. Hazard. Mater. 154 (2007) 73–78.
[15] M.A. Al-Ghouti, M.A.M. Khraisheh, M.N.M. Ahmad, S. Allen, Adsorption behaviour of methylene blue onto Jordanian diatomite: A kinetic study, J. Hazard. Mater. 165 (2009) 589–598.
[16] R.A. Shawabkeh, M.F. Tutunji, Experimental study and modeling of basic dye sorption by diatomaceous clay, Appl. Clay Sci. 24 (2003) 111–120.
[17] E. Erdem, G. Çölgeçen, R. Donat, The removal of textile dyes by diatomite earth, J. Colloid Interface Sci. 282 (2005) 314–319.
[18] Y. Al-Degs, M.A. Khraisheh, M.F. Tutunji, Sorption of lead ions on diatomite and manganese oxides modified diatomite, Water Res. 35 (2001) 3724–3728.
[19] M. Gürü, D. Venedik, A. Murathan, Removal of trivalent chromium from water using low-cost natural diatomite, J. Hazard. Mater. 160 (2008) 318–323.
[20] A.F. Danil de Namor, A. El Gamouz, S. Frangie, V. Martinez, L. Valiente, O.A. Webb, Turning the volume down on heavy metals using tuned diatomite. A review of diatomite and modified diatomite for the extraction of heavy metals from water, J. Hazard. Mater. 241-242 (2012) 14–31.
[21] M.A.M. Khraisheh, Y.S. Aldegs, W.A.M. Mcminn, Remediation of wastewater containing heavy metals using raw and modified diatomite, Chem. Eng. J. 99 (2004) 177–184.
[22] K. Badii, F.D. Ardejan, M.A. Saberi, N.Y. Limaee, S.Z. Shafaei, Adsorption of Acid blue 25 dye on diatomite in aqueous solutions, Indian J. Chem. Technol. 17 (2010) 7–16.
[23] Y.S. Al-Degs, M.F. Tutunju, R.A. Shawabkeh, The feasibility of using diatomite and Mn–diatomite for remediation of Pb^{2+} , Cu^{2+} , and Cd^{2+} from water, Sep. Sci. Technol. 35 (2000) 2299–2310.
[24] T.N. De Castro-Dantas, A.A. Neto, M.C. De A. Moura, Removal of chromium from aqueous solutions by diatomite treated with microemulsion, Water Res. 35 (2001) 2219–2224.
[25] P. Miretzky, C. Muñoz, E. Cantoral-Uriza, $Cd2^{+}$ adsorption on alkaline-pretreated diatomaceous earth: equilibrium and thermodynamic studies, Environ. Chem. Lett. 9 (2011) 55–63.
[26] Jang M., S.H. Min, J. Park, E.J. Tlachac, Hydrous ferric oxide incorporated diatomite for remediation of arsenic contaminated groundwater. Environ. Sci. Technol. 41 (2007) 3322–3328.
[27] M. Al-Ghouti, M.A.M. Khraisheh, M.N.M. Ahmad, S. Allen, Thermodynamic behaviour and the effect of temperature on the removal of dyes from aqueous solution using modified diatomite: A kinetic study, J. Colloid Interface Sci. 287 (2005) 6–13.
[28] Z. Al-Qodah, W.K. Lafi, Z. Al-Anber, M. Al-Shannag, A. Harahsheh, Adsorption of methylene blue by acid and heat treated diatomaceous silica, Desalination 217 (2007) 212–224.
[29] H. Hadjar, B. Hamdi, M. Jaber, J. Brendlé, Z. Kessaïssia, H. Balard, J.B. Donnet, Elaboration and characterisation of new mesoporous materials from diatomite and charcoal, Microporous Mesoporous Mater. 107 (2008) 219–226.
[30] H. Hadjar, B. Hamdi, Z. Kessasia, Adsorption of heavy metal ions on composite materials prepared by modification of natural silica, Desalination 167 (2004) 165–174.
[31] H. Hadjar, B. Hamdi, C.O. Ania, Adsorption of p-cresol on novel diatomite/carbon composites, J. Hazard. Mater. 188 (2011) 304–310.
[32] R.C. Bansal, J.B. Donnet, F. Stoeckli, Active Carbon, Marcel Dekker, New York, NY, 1998.
[33] A. Warhurst, G.D. Fowler, G.L. McConnachie, S.J.T. Pollard, Pore structure and adsorption characteristics of steam pyrolysis carbons from *Moringa oleifera*, Carbon 35 (1997) 1039–1045.
[34] H. Alyosef, S. Ibrahim, J. Welscher, A. Inayat, A. Eilert, R. Denecke, W. Schwieger, T. Münster, G. Kloess, W.D. Einicke, D. Enke, Effect of acid treatment on the chemical composition and the structure of Egyptian diatomite. Int. J. Miner. Process. 132 (2014) 17–25.
[35] B. Al-Duri, Introduction to adsorption. in: G. McKay (Ed.), Use of Adsorbents for the Removal of Pollutants from Wastewaters, CRC Press, Boca Raton, FL, 1996, pp. 1–6.
[36] M. Sprynskyy, I. Kovalchuk, B. Buszewski, The separation of uranium ions by natural and modified diatomite from aqueous solution, J. Hazard. Mater. 181 (2010) 700–707.
[37] G.S. Deshmukh, S.U. Pathak, D. Peshwe, J.D. Ekhe, Effect of uncoated calcium carbonate and stearic acid coated calcium carbonate on mechanical, thermal and structural properties of poly(butylene terephthalate) (PBT)/calcium carbonate composites, Bull. Mater. Sci. 33 (2010) 277–284.
[38] G. Sheng, H. Dong, H. Li, Characterization of diatomite and its application for the retention of radiocobalt: Role of environmental parameters, J. Environ. Radioact. 113 (2010) 108–115.
[39] G. Sheng, J. Hu, X. Wang, Sorption properties of Th (IV) on the raw diatomite—Effects of contact time, pH, ionic strength and temperature, Appl. Radiat. Isot. 66 (2008) 1313–1320.
[40] M. Sprynskyy, R. Gadzała-Kopciuch, K. Nowak, B. Buszewski, Removal of zearalenone toxin from synthetics gastric and body fluids using talc and diatomite: A batch kinetic study, Colloids Surf., B 94 (2012) 7–14.
[41] P.M. Álvarez, J.F. García-Araya, F.J. Beltrán, F. Masa, F. Medina, Ozonation of activated carbons: Effect on the adsorption of selected phenolic compounds from aqueous solutions, J. Colloid Interface Sci. 283 (2005) 503–512.
[42] D. Liu, W. Yuan, L. Deng, W. Yu, H. Sun, P. Yuan, Preparation of porous diatomite-templated carbons with large adsorption capacity and mesoporous zeolite K-H as a byproduct, J. Colloid Interface Sci. 424 (2014) 22–26.

[43] A. Bakandritsos, T. Steriotis, D. Petridis, High surface area montmorillonite−Carbon composites and derived carbons, Chem. Mater. 16 (2004) 1551–1559.
[44] P.M. Barata-Rodrigues, T.J. Mays, G.D. Moggridge, Structured carbon adsorbents from clay, zeolite and mesoporous aluminosilicate templates, Carbon 41 (2003) 2231–2246.
[45] M. Aivalioti, I. Vamvasakis, E. Gidarakos, BTEX and MTBE adsorption onto raw and thermally modified diatomite, J. Hazard. Mater. 178 (2010) 136–143.
[46] M.A.M. Khraisheh, M.A. Al-Ghouti, S.J. Allen, M.N. Ahmad, Effect of OH and silanol groups in the removal of dyes from aqueous solution using diatomite, Water Res. 39 (2005) 922–932.
[47] M. Aivalioti, P. Papoulias, A. Kousaiti, E. Gidarakos, Adsorption of BTEX, MTBE and TAME on natural and modified diatomite, J. Hazard. Mater. 207-208 (2012) 117–127.
[48] W.T. Tsai, K.J. Hsien, Y.M. Chang, C.C. Lo, Removal of herbicide paraquat from an aqueous solution by adsorption onto spent and treated diatomaceous earth, Bioresour. Technol. 96 (2011) 657–663.
[49] G. McKay, Y.S. Ho, Pseudo second-order model for sorption processes, Process Biochem. 34 (1999) 451–465.
[50] L. Zhuang, G. Wang, K. Yu, C. Yao, Enhanced adsorption of anionic dyes from aqueous solution by gemini cationic surfactant-modified diatomite, Desalin. Water Treat. 51 (2013) 6526–6535.
[51] F. Rozada, M. Otero, A. Moran, A. Garcia, Activated carbons from sewage sludge and discarded tyres: Production and optimization, J. Hazard. Mater. 124 (2005) 181–191.
[52] C.H. Giles, T.H. MacEwan, S.N. Nakhwa, D. Smith, 786. Studies in adsorption. Part XI. A system of classification of solution adsorption isotherms, and its use in diagnosis of adsorption mechanisms and in measurement of specific surface areas of solids. J. Chem. Soc. 786 (1960) 3973–3993.
[53] I. Langmuir, The constitution and fundamental properties of solids and liquids. Part I. Solids, Am. Chem. Soc. 38 (1916) 2221–2295.
[54] Y.S. Ho, G. Mckay, Kinetic models for the sorption of dye from aqueous solution by wood, Trans. IChemE. 76 (1998) 183–191.
[55] A.E. Ofomaja, Kinetics and mechanism of methylene blue sorption onto palm kernel fibre, Process Biochem. 42 (2007) 16–24.